

Seismic and geodetic evidence for extensive, long-lived fault damage zones

Elizabeth S. Cochran¹, Yong-Gang Li², Peter M. Shearer³, Sylvain Barbot³, Yuri Fialko³, John E. Vidale⁴

¹Department of Earth Sciences, University of California–Riverside, Riverside, California 92521, USA

²Department of Earth Sciences, University of Southern California, Los Angeles, California 90089, USA

³Institute of Geophysics and Planetary Physics, Scripps Institution of Oceanography, University of California–San Diego, La Jolla, California 92093, USA

⁴Department of Earth and Space Sciences, University of Washington, Seattle, Washington 98195, USA

ABSTRACT

During earthquakes, slip is often localized on preexisting faults, but it is not well understood how the structure of crustal faults may contribute to slip localization and energetics. Growing evidence suggests that the crust along active faults undergoes anomalous strain and damage during large earthquakes. Seismic and geodetic data from the Calico fault in the eastern California shear zone reveal a wide zone of reduced seismic velocities and effective elastic moduli. Using seismic traveltimes, trapped waves, and interferometric synthetic aperture radar observations, we document seismic velocities reduced by 40%–50% and shear moduli reduced by 65% compared to wall rock in a 1.5-km-wide zone along the Calico fault. Observed velocity reductions likely represent the cumulative mechanical damage from past earthquake ruptures. No large earthquake has broken the Calico fault in historic time, implying that fault damage persists for hundreds or perhaps thousands of years. These findings indicate that faults can affect rock properties at substantial distances from primary fault slip surfaces, and throughout much of the seismogenic zone, a result with implications for the amount of energy expended during rupture to drive cracking and yielding of rock and development of fault systems.

INTRODUCTION

Previous seismic studies have suggested that fault damage zones are only a few hundred meters wide. Studies along the 1992 M_w 7.3 Landers, California, earthquake, the 1999 M_w 7.1 Hector Mine, California, earthquake, and the 1999 M_w 7.4 Izmit, Turkey, earthquake characterized the fault damage regions as zones 100–200 m wide with seismic velocity reductions of 20%–40% (Vidale and Li, 2003; Li et al., 1998; Ben-Zion et al., 2003). A study of the 2004 M_w 6.0 Parkfield earthquake showed shear wave velocities in a 200-m-wide damage zone were further reduced 1.0%–1.5%, with recovery of seismic velocities observable in subsequent months (Li et al., 2006). Fault damage zone healing has also been reported in the years to decades following a mainshock (Vidale and Li, 2003; Li et al., 1998). However, it is not known if fault zone damage persists over a full earthquake cycle, which may last hundreds to thousands of years. Thus, understanding the fault zone structure and degree of damage along a major crustal fault has implications for localization of strain, triggering of earthquakes, and the mechanics of earthquake rupture. Here we combine seismic and geodetic data from the eastern California shear zone Calico fault, which has remained unbroken in historical time, to probe the structure and long-term properties of fault damage zones.

The Calico fault is located midway between the 1992 M_w 7.3 Landers and 1999 M_w 7.1 Hector Mine ruptures (Fig. 1A). The northwest-striking Calico fault has accumulated ~10 km of dextral slip since its inception (Dokka and Travis, 1990; Oskin et al., 2007). The Calico fault has the highest average dextral slip rate within the eastern California shear zone, ~1–2 mm/yr (Dokka and Travis, 1990; Oskin et al., 2007), and some geodetic estimates suggest higher slip rates, as much as 7 mm/yr (Peltzer et al., 2001). Earthquakes on the Mojave Desert portion of the eastern

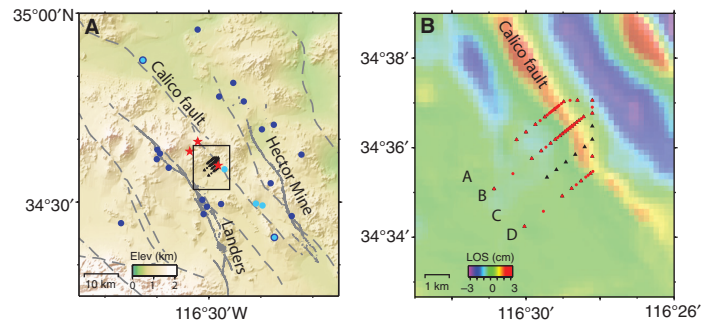


Figure 1. Overview map of station and event distribution. A: Shaded relief map of Mojave Desert region. Regional faults are shown by dashed gray lines, and Landers and Hector Mine ruptures are shown by solid gray lines. Light and dark blue circles indicate local earthquakes used in the fault zone trapped wave and traveltimes analyses, respectively. Light blue circles with dark blue outline were used in both analyses. Red stars denote shots. Black triangles and circles show seismic stations. Gray square outlines region in B. B: High-pass-filtered coseismic interferogram from the 16 October 1999 Hector Mine earthquake that spans period from 13 January–20 October 1999 (after Fialko et al., 2002). Colors denote variations in line of sight (LOS) displacements. Black triangles and red circles are intermediate-period and short-period seismic stations.

California shear zone faults have extremely long recurrence times of a few thousand years (Rubin and Sieh, 1997), but are inferred to cluster in time (Rockwell et al., 2000). While paleoseismic studies on the Calico fault are sparse, recent trench data indicate that the last earthquake occurred at least several hundred years ago (Ganev et al., 2008).

Coseismic interferograms for both the Landers and Hector Mine earthquakes showed strain localized on the Calico fault as well as on other nearby faults (Fialko et al., 2002; Fialko, 2004). Line-of-sight displacements with amplitudes of a few centimeters and wavelengths of a few kilometers are clearly associated with the Calico fault trace (Fig. 1B). Initial interpretation of the interferometric synthetic aperture radar (InSAR) anomalies for the Calico fault suggested triggered slip (Sandwell et al., 2000), but this required left-lateral movement opposite to the long-term motion. An alternative interpretation held that the InSAR observations are best explained with a 1–2-km-wide zone around the fault with a shear modulus reduced by 50% extending to at least 5 km depth (Fialko et al., 2002). These geodetic results suggest a fault zone width (~2 km) an order of magnitude greater than generally reported for low-velocity zones on major faults determined using seismic data (200 m) (Li et al., 1998, 2006; Ben-Zion et al., 2003; Mamada et al., 2004; McGuire and Ben-Zion, 2005).

DATA ANALYSIS

We conducted a detailed seismic investigation of the Calico fault to test the interpretation of the anomalous strain detected by InSAR as elastic deformation of compliant zones in response to coseismic loading, and to

determine if the variations in static moduli observed with InSAR are similar to dynamic moduli variations observed with seismic data. We installed a dense array of 40 intermediate period stations and 60 short-period stations in a 1.5 km × 5.5 km grid adjacent to the Calico fault (Fig. 1B). We detonated three shots and recorded background seismicity for six months. We applied three independent methods to determine the fault structure of the Calico fault: (1) finite-difference modeling of fault zone–trapped waves, (2) traveltimes modeling of P arrival times, and (3) static stress modeling of the compliant zone in response to the Landers and Hector Mine earthquakes.

Fault zone–trapped waves are seismic waves confined within the low-velocity structure adjacent to the fault that are excited by earthquakes or explosions located within the fault zone. Thus, the trapped wave analysis is limited to events that occurred on or relatively close to the Calico fault; here we present results derived from two shots and five local earthquakes (see the GSA Data Repository¹). Full synthetic waveforms are computed for each event station pair using a three-dimensional (3-D) finite-difference scheme and compared to actual waveforms (Fig. 2). We vary the damage zone width, depth, and velocity reduction to determine the best fit to the data. The width of the zone is controlled mostly by the observation of high-amplitude trapped waves following the S arrival on stations near the fault trace. If the damage zone extends across the seismogenic zone, the envelope of the trapped wave will have a longer duration for deeper earthquakes. For the deepest on-fault earthquake, at a depth of 10.8 km, we see a clear increase in the duration of the trapped wave energy envelope.

Traveltimes analysis allows us to map the seismic velocities across the grid of seismic stations. The velocity reduction within the Calico fault damage zone is substantial, as indicated by delays in the body wave arrivals near the fault (Fig. 3). We do not have sufficient ray coverage to perform a tomographic inversion for the 3-D velocity structure under our array; instead we determine the fault zone models that best fit the P arrivals from shots and earthquakes (Fig. 1). Events chosen for this study were well recorded by the array, have good signal-to-noise ratios, and cover a range of back azimuths to best image the entire fault zone. We modeled three shots, 20 local earthquakes, and eight teleseismic earthquakes. We compute traveltimes based on the graph theory technique of Moser (1991), modified as described in Nolet et al. (2005), to get stable results for the strong 3-D velocity variations in our models.

RESULTS

The best-fit fault models were initially determined independently for the fault zone trapped wave, traveltimes, and InSAR data sets. The model results for the three data sets were surprisingly consistent, so we fit all of the data to a single model (see the Data Repository) (Fig. 4A). We find that the fault zone is ~1.5 km wide with a P-wave velocity reduction of ~40%, with similar misfits seen in a range between 30% and 50%. There is some trade-off between the velocity reduction and the width of the fault; models with fault zone widths between 1 and 2 km fit the data with nearly the same misfit. The lateral velocity profile across the fault is approximated as a Hanning taper, and the velocity reduction tapers linearly to zero between 0 and 12 km depth.

The damage zone is modeled to extend to 12 km depth, but with small relative velocity reductions below ~5 km (Fig. 4A). Synthetic waveforms are well fit to the fault zone trapped wave data (Fig. 2), showing a clear increase in trapped energy within 750 m of the fault trace. Modeled and actual traveltimes plots show similar width and amplitude for the velocity anomaly along the Calico fault (Fig. 3). The depth of the zone

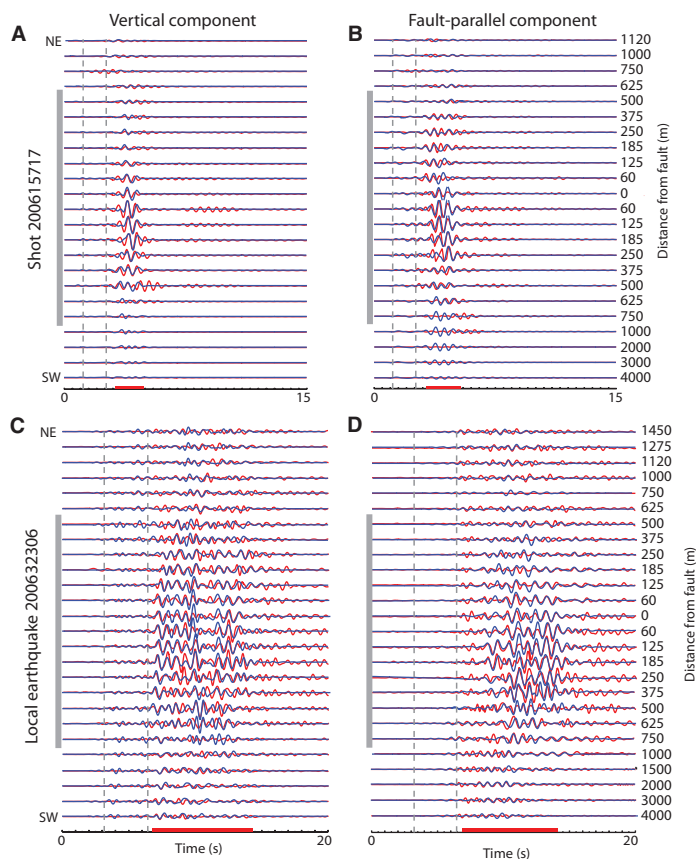


Figure 2. Recorded and synthetic fault zone trapped wave data. A: Recorded (red) and synthetic (blue) vertical seismograms for shot 200615717. Vertical dashed lines indicate the P and S wave arrivals. Red bar indicates approximate timing of strong trapped wave energy. Width of compliant zone is shown by vertical gray bar (~1.5 km wide). Synthetic seismograms were computed using model shown in Figure 4 with an S velocity reduction of 50% as described in text. B: Recorded (red) and synthetic (blue) fault-parallel seismograms for shot 200615717. C: Recorded (red) and synthetic (blue) vertical seismograms for local earthquake 200632306. D: Recorded (red) and synthetic (blue) fault-parallel seismograms for local earthquake 200632306. Data are low-pass filtered at 2 Hz.

is constrained by a single near-fault earthquake, located 27.9 km away and 10.8 km deep, with extended trapped wave energy that cannot be matched using a model with a shallow damage zone (see the Data Repository).

To test whether the seismically imaged fault zone is consistent with available geodetic data, we modeled the response of the best-fitting compliant structure (Fig. 4A) to static stress changes due to the Landers and Hector Mine earthquakes. We converted the seismic velocity model (Fig. 4A) into elastic moduli assuming a constant density. The resulting 2-D variations in elastic moduli were extrapolated along the Calico fault to obtain a 3-D fault zone model. A similar compliant structure was also introduced around the nearby Rodman fault. We calculated the coseismic deformation due to the compliant zones using the equivalent body force method in the spectral domain (Barbot et al., 2008). Figure 4B shows the observed displacements in the satellite line of sight across the Calico fault and predictions for the best-fitting seismic tomography model. The modeled response of the Calico fault zone is in good agreement with InSAR data, indicating that the same variations in moduli between the fault zone and the ambient crust can account for both the static (geodetic) and dynamic (seismic) deformation. The InSAR data cannot be fit with a shallow compliant zone and thus provide an additional constraint on the

¹GSA Data Repository item 2009082, seismic and geodetic data analysis and modeling methods, is available online at www.geosociety.org/pubs/ft2009.htm, or on request from editing@geosociety.org or Documents Secretary, GSA, P.O. Box 9140, Boulder, CO 80301, USA.

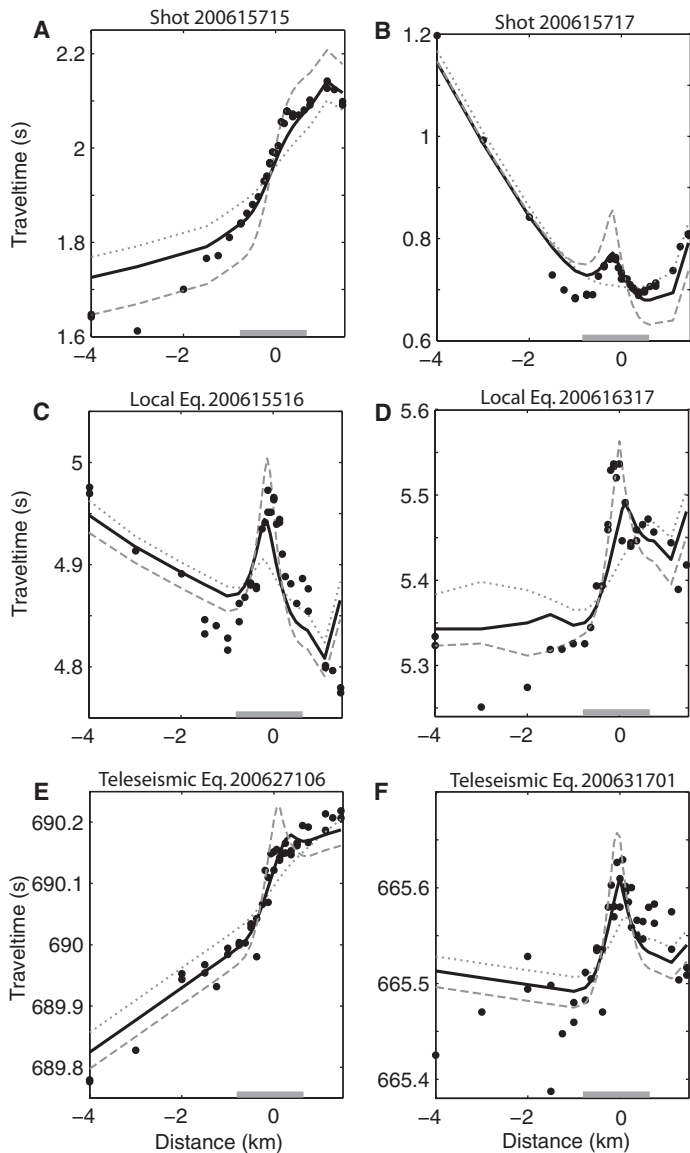


Figure 3. Traveltime data and forward model comparison. Examples of fits of several models with different velocity reductions (lines) to the traveltime data (points) across line B (see Fig. 1). Fault zone geometry is shown in Figure 4. Models shown are 10% velocity reduction (dotted gray line), 40% velocity reduction (solid black line), and 70% velocity reduction (dashed gray line). Solid line denotes preferred model as described in text. Data are shown for events. A: Shot 200615715. B: Shot 200615717. C: Local earthquake (Eq.) 200615516. D: Local earthquake 200616317. E: Teleseismic earthquake 200627106. F: Teleseismic earthquake 200631701. Gray bar represents modeled 1.5 km width of low-velocity zone.

fault zone depth. Both the InSAR and fault zone trapped waves indicate that the damage zone likely extends to at least 5 km depth, but is narrower and with a lower velocity contrast at greater depths.

DISCUSSION

As documented here, we observe a 1.5-km-wide zone with seismic wave velocities reduced up to 40%–50% and a shear modulus reduced by 65% along the Calico fault. This zone likely represents a region of mechanically weakened, or damaged, rocks related to the cumulative effect of past ruptures (Fig. 4B). The damage zone imaged along the Calico fault is much wider than those reported by previous seismic observations on

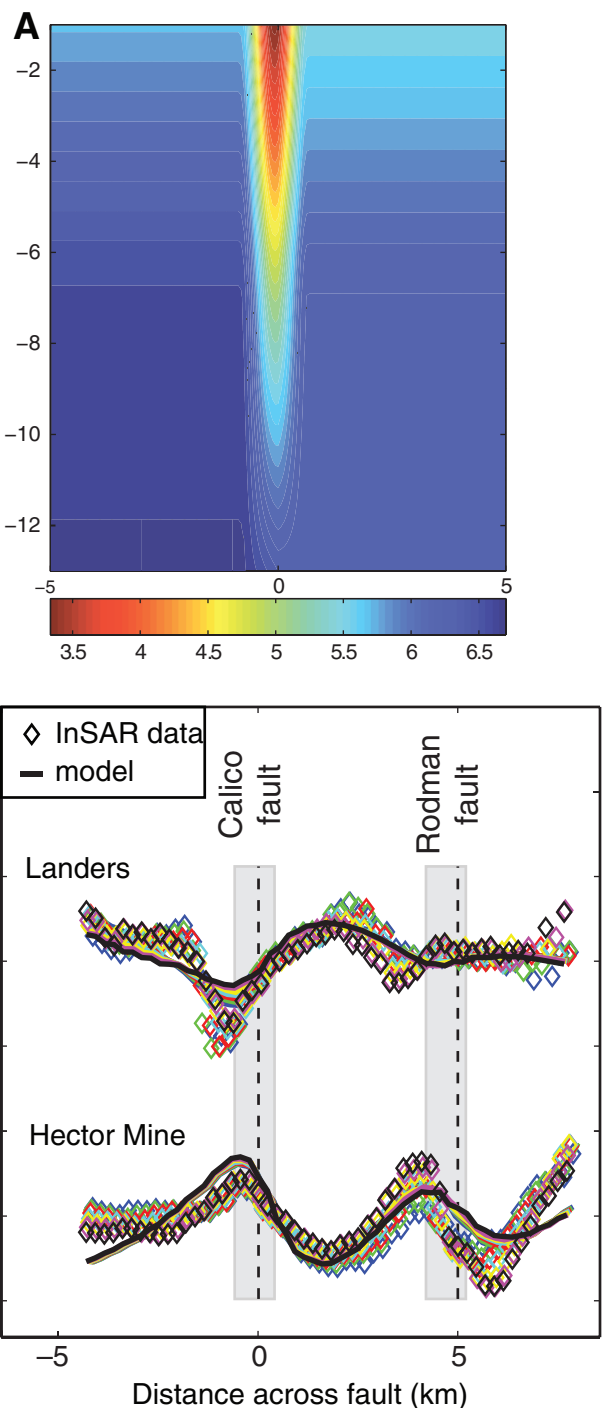


Figure 4. Best-fit model and interferometric synthetic aperture radar (InSAR) model and data. A: Model of P-wave low-velocity zone along Calico fault with 40% reduction in velocity. Additional parameters are described in text. B: Observed line of sight (LOS) displacements across Calico fault (color diamonds) and predictions for best-fitting model using geometry shown in A, but with v reduced by 65% and λ reduced by 30%. Color diamonds represent different swaths perpendicular to the Calico fault.

neighboring faults, 1.5 km versus 200 m. This apparent discrepancy might result because most seismic studies of fault zones were initiated following a large mainshock (Vidale and Li, 2003; Li et al., 1998, 2006; Ben-Zion et al., 2003) rather than late in the interseismic period. These studies focused on narrow zones that may be more highly damaged immediately

following a large earthquake, but heal subsequently. Perhaps most important, most previous studies did not deploy arrays at great enough distances from the fault to see the wide damage zone implied here. These studies may not have seen the true edge of the fault zone, but were comparing the highly damaged portion of the fault to the less damaged region 200–300 m from the main slip plane.

Some geologic studies have also indicated that fault deformation zones can extend to greater distances from the main slip plane. An aftershock study concluded that the Landers rupture has a 300-m-wide low-velocity zone that extends to at least 7 km depth (Li et al., 2007), where previous studies indicated only a 180-m-wide zone (Li et al., 1998). A wide (1–2 km) damage zone was inferred on the Calaveras fault from observations of fault zone trapped waves on a widely spaced array (Spudich and Olsen, 2001). Oskin et al. (2007) reported deflection of the Silver Bell fault by distributed shear adjacent to the Calico fault over a width comparable to the damage zone imaged here.

Differences in the inferred widths of compliant zones may also be due to intrinsic variations in the width of damaged zones around different faults, as well as along different sections of the same fault. Substantial changes in the effective width of the compliant zone of the Calico fault along strike are apparent in the InSAR line-of-sight displacements. Observations using dense geodetic networks revealed several localized zones of high interseismic strain along the San Andreas fault that were attributed to compliant fault zones (Lisowski et al., 1991; Chen and Freymueller, 2002). Detailed mapping of near-field interseismic deformation may provide further insights into the ubiquity and spatial variability of permanent damage around active faults.

Results presented in this study indicate that faults can affect rock properties at greater distances than generally documented. The observed reduction in the elastic rigidity of a wide zone surrounding the primary slip surface is likely a result of wall-rock fracturing and yielding during earthquakes. Quantifying the degree and spatial extent of fault zone damage provides constraints on the portion of fracture energy expended during rupture (e.g., Fialko, 2007). A wide, persistent compliant zone along a fault identifies a region that is most likely weaker than the surrounding rock, facilitating the localization of regional strain. Strain localization leads to faults that are more responsive to relatively small stress changes, thus enhancing the tendency for earthquakes to rupture well-established faults rather than more intact rock. Permanent damage zones may thus play a critical role in the development and dynamics of faults, fault systems, and plate boundaries.

ACKNOWLEDGMENTS

We thank all of the field volunteers for their hard work under the blazing Mojave sun. We thank Guust Nolet for providing ray tracing software. We also thank Mike Oskin and an anonymous reviewer for their constructive comments on the paper. This research was supported by the National Science Foundation (grant EAR-0439947) and the Southern California Earthquake Center (contribution 1185).

REFERENCES CITED

Barbot, S., Fialko, Y., and Sandwell, D., 2008, Effect of a compliant fault zone on the inferred earthquake slip distribution: *Journal of Geophysical Research*, v. 113, B06404, doi: 10.1029/2007JB005256.

Ben-Zion, Y., Peng, Z., Okaya, D., Seeber, L., Armbruster, J.G., Ozer, N., Michael, A.J., Baris, S., and Aktar, M., 2003, A shallow fault-zone structure illuminated by trapped waves in the Karadere-Duzce branch of the North Anatolian Fault, western Turkey: *Geophysical Journal International*, v. 152, p. 699–717, doi: 10.1046/j.1365-246X.2003.01870.x.

Chen, Q., and Freymueller, J., 2002, Geodetic evidence for a near-fault compliant zone along the San Andreas fault in the San Francisco bay area: *Seismological Society of America Bulletin*, v. 92, p. 656–671, doi: 10.1785/0120010110.

Dokka, R.K., and Travis, C.J., 1990, Late Cenozoic strike-slip faulting in the Mojave Desert, California: *Tectonics*, v. 9, p. 311–340, doi: 10.1029/TC009i002p00311.

Fialko, Y., 2004, Probing the mechanical properties of seismically active crust with space geodesy: Study of the coseismic deformation due to the 1992 M w 7.3 Landers (southern California) earthquake: *Journal of Geophysical Research*, v. 109, B03307, doi: 10.1029/2003JB002756.

Fialko, Y., 2007, Fracture and frictional mechanics—Theory, in Kanamori, H., ed., *Earthquake seismology: Treatise on Geophysics*, Volume 4: London, Elsevier, p. 83–106.

Fialko, Y., Sandwell, D., Agnew, D., Simons, M., Shearer, P., and Minster, B., 2002, Deformation on nearby faults induced by the 1999 Hector Mine earthquake: *Science*, v. 297, p. 1858–1862, doi: 10.1126/science.1074671.

Ganev, P.N., Dolan, J.F., Oskin, M.E., Owen, L.A., and Le, K.N., 2008, Paleoseismologic evidence for multiple Holocene earthquakes on the Calico fault: Implications for earthquake clustering in the eastern California shear zone: *Southern California Earthquake Center Annual Meeting Proceedings and Abstracts*, v. XVIII, p. 153–154.

Li, H., Zhu, L., and Yang, H., 2007, High-resolution structures of the Landers fault zone inferred from aftershock waveform data: *Geophysical Journal International*, v. 171, p. 1295–1307.

Li, Y.-G., Vidale, J.E., Aki, K., Xu, F., and Burdette, T., 1998, Evidence of shallow fault zone strengthening after the 1992 M7.5 Landers, California, earthquake: *Science*, v. 279, p. 217–219, doi: 10.1126/science.279.5348.217.

Li, Y.-G., Chen, P., Cochran, E.S., Vidale, J.E., and Burdette, T., 2006, Seismic evidence for rock damage and healing on the San Andreas Fault associated with the 2004 M 6.0 Parkfield earthquake: *Seismological Society of America Bulletin*, v. 96, p. S349–S363, doi: 10.1785/0120050803.

Lisowski, M., Savage, J.C., and Prescott, W.H., 1991, The velocity field along the San Andreas fault in central and southern California: *Journal of Geophysical Research*, v. 96, p. 8369–8389, doi: 10.1029/91JB00199.

Mamada, Y., Kuwahara, Y., Ito, H., and Takenaka, H., 2004, Discontinuity of the Mozumi-Sukenobu fault low-velocity zone, central Japan, inferred from 3-D finite-difference simulation of fault zone waves excited by explosive sources: *Tectonophysics*, v. 378, p. 209–222, doi: 10.1016/j.tecto.2003.09.008.

McGuire, J., and Ben-Zion, Y., 2005, High-resolution imaging of the Bear Valley section of the San Andreas fault at seismogenic depths with fault-zone head waves and relocated seismicity: *Geophysical Journal International*, v. 163, p. 152–164, doi: 10.1111/j.1365-246X.2005.02703.x.

Moser, T.J., 1991, Shortest path calculation of seismic rays: *Geophysics*, v. 56, p. 59–67, doi: 10.1190/1.1442958.

Nolet, G., Dahlen, F.A., and Montelli, R., 2005, Traveltimes and amplitudes of seismic waves: A re-assessment, in Levander, A., and Nolet, G., eds., *Array analysis of broadband seismograms: American Geophysical Union Geophysical Monograph 157*, p. 37–48.

Oskin, M., Peng, L., Blumentritt, D., Mukhopadhyay, S., and Iriondo, A., 2007, Slip rate of the Calico fault: Implications for geologic versus geodetic rate discrepancy in the eastern California shear zone: *Journal of Geophysical Research*, v. 112, B03402, doi: 10.1029/2006JB004451.

Peltzer, G., Crampe, F., Hensley, S., and Rosen, P., 2001, Transient strain accumulation and fault interaction in the Eastern California shear zone: *Geology*, v. 29, p. 975–978, doi: 10.1130/0091-7613(2001)029<0975:TSAAFI>2.0.CO;2.

Rockwell, T.K., Lindvall, S., Herzberg, M., Murbach, D., Dawson, T., and Berger, G., 2000, Paleoseismology of the Johnson Valley, Kickapoo, and Homestead Valley faults: Clustering of earthquakes in the eastern California shear zone: *Seismological Society of America Bulletin*, v. 90, p. 1200–1236, doi: 10.1785/0119990023.

Rubin, C., and Sieh, K., 1997, Long dormancy, low slip rate, and similar slip-per-event for the Emerson fault, eastern California shear zone: *Journal of Geophysical Research*, v. 102, p. 15,319–15,333.

Sandwell, D.T., Sichoix, L., Agnew, D., Bock, Y., and Minster, J.-B., 2000, Near real-time radar interferometry of the Mw 7.1 Hector Mine earthquake: *Geophysical Research Letters*, v. 27, p. 3101–3104, doi: 10.1029/1999GL011209.

Spudich, P., and Olsen, K., 2001, Fault zone amplified waves as a possible seismic hazard along the Calaveras fault in Central California: *Geophysical Research Letters*, v. 28, p. 2533–2536, doi: 10.1029/2000GL011902.

Vidale, J.E., and Li, Y.-G., 2003, Damage to the shallow Landers fault from the nearby Hector Mine earthquake: *Nature*, v. 421, p. 524–526, doi: 10.1038/nature01354.

Manuscript received 17 July 2008

Revised manuscript received 10 November 2008

Manuscript accepted 16 November 2008

Printed in USA